Science Bulletin 62 (2017) 1494–1496

Contents lists available at ScienceDirect

Science Bulletin

journal homepage: www.elsevier.com/locate/scib

Short Communication

26 mA cm^{-2} J_{sc} from organic solar cells with a low-bandgap nonfullerene acceptor

Zuo Xiao [a,1], Xue Jia [a,1], Dan Li [a,b], Shizhe Wang [a], Xinjian Geng [a], Feng Liu [c,*], Junwu Chen [d,*], Shangfeng Yang [b,*], Thomas P. Russell [e], Liming Ding [a,*]

[a] *Center for Excellence in Nanoscience (CAS), Key Laboratory of Nanosystem and Hierarchical Fabrication (CAS), National Center for Nanoscience and Technology, Beijing 100190, China*
[b] *Department of Materials Science and Engineering, University of Science and Technology of China, Hefei 230026, China*
[c] *Department of Physics and Astronomy, Shanghai Jiaotong University, Shanghai 200240, China*
[d] *State Key Laboratory of Luminescent Materials and Devices, South China University of Technology, Guangzhou 510640, China*
[e] *Department of Polymer Science and Engineering, University of Massachusetts, Amherst, MA 01003, USA*

ARTICLE INFO

Article history:
Received 3 October 2017
Received in revised form 11 October 2017
Accepted 11 October 2017
Available online 26 October 2017

Nonfullerene-based organic solar cells (NFOSCs) have received great interest recently due to their higher performance and greater potential compared with fullerene-based solar cells [1]. Power conversion efficiencies (PCEs) over 13% have been realized in single-junction NFOSCs [2]. Compared with traditional fullerene acceptors, the greatest advantage of nonfullerene acceptors is their stronger light-harvesting capability in the visible and near-infrared (NIR) regions, which helps to generate high photocurrent for solar cells. By assembling a carbon-bridged ladder-type electron-donating unit (D), such as indacenodithiophene (IDT), with two electron-accepting end groups (A), such as 1,1-dicyanomethylene-3-indanone (IC), Zhan and co-workers [3] developed a series of highly efficient A-D-A type small molecule acceptors. These acceptors generally show low optical bandgaps ($E_{\mathrm{g}}^{\mathrm{opt}}$) and strong absorbance in NIR region. Blending them with absorption-complementary and energy-level-matching D-A copolymer donors can realize very high short-circuit current density (J_{sc}) in organic solar cells. Recently, a 25.3 mA cm^{-2} J_{sc} record was achieved from a ternary-blend cell, containing a low-bandgap A-D-A acceptor, IEICO-4F ($E_{\mathrm{g}}^{\mathrm{opt}} = 1.24$ eV), and two D-A copolymers, PTB7-Th and J52 [4]. Low-bandgap A-D-A acceptors demonstrated great potential in tandem cells [5] and semi-transparent cells [6]. Low-bandgap A-D-A acceptors are promising materials for organic solar cells.

Increasing the electron-donating capability of D unit or/and the electron-accepting capability of A unit is an effective strategy to lower the bandgap of A-D-A acceptors. We have reported a novel carbon-oxygen-bridged ladder-type D unit, CO5 [7]. Inserting electron-rich oxygen atoms into the backbone not only improves the electron-donating capability of the unit but also expands backbone planarity. As a result, CO5 shows enhanced electron-donating capability and planarity than the carbon-bridged analogue IDT. The A-D-A acceptor CO5IC shows a narrower bandgap, stronger light-harvesting capability, higher electron mobility and better photovoltaic performance than IDTIC (Fig. 1a). However, 1.62 eV $E_{\mathrm{g}}^{\mathrm{opt}}$ of CO5IC is still relatively high. To reduce $E_{\mathrm{g}}^{\mathrm{opt}}$ and achieve higher performance in solar cells, we designed a low-bandgap A-D-A acceptor, CO$_i$8DFIC, in this work. First, a new carbon-oxygen-bridged unit, CO$_i$8, was developed and used as D unit. "*i*" indicates that C—O bond points to the core of the molecule and "8" stands for eight fused rings. Compared with CO5, CO$_i$8 possesses higher electron-donating capability due to three electron-richer thienothiophene moieties. Second, a stronger electron-accepting unit, difluoro-substituted IC (DFIC), was used as the end groups. The enhanced electron-donating capability and electron-accepting capability lead to a very small $E_{\mathrm{g}}^{\mathrm{opt}}$ (1.26 eV) for CO$_i$8DFIC. The enhanced planarity also renders CO$_i$8DFIC good charge-transporting property. CO$_i$8DFIC exhibits outstanding performance in NFOSCs. A J_{sc} of 26.12 mA cm^{-2} and a decent PCE of 12.16% were achieved from PTB7-Th:CO$_i$8DFIC solar cells.

The synthetic route for CO$_i$8DFIC is shown in Scheme S1 (online). 3,6-Dimethoxythieno[3,2-*b*]thiophene was transformed into (3,6-dimethoxythieno[3,2-*b*]thiophene-2,5-diyl)bis(trimethylstannane) in 76% yield. Stille coupling of the organoditin compound with ethyl 2-bromothieno[3,2-*b*]thiophene-3-carboxylate gave compound **1** in 89% yield. Treating compound **1** with BBr_3 afforded the demethylated compound **2** in 100% yield. Then, compound **2** was quantitatively converted to bislactone **3** via an

---

* Corresponding authors.
E-mail addresses: fengliu82@sjtu.edu.cn (F. Liu), psjwchen@scut.edu.cn (J. Chen), sfyang@ustc.edu.cn (S. Yang), ding@nanoctr.cn (L. Ding).

[1] These authors contributed equally to this work.

https://doi.org/10.1016/j.scib.2017.10.017

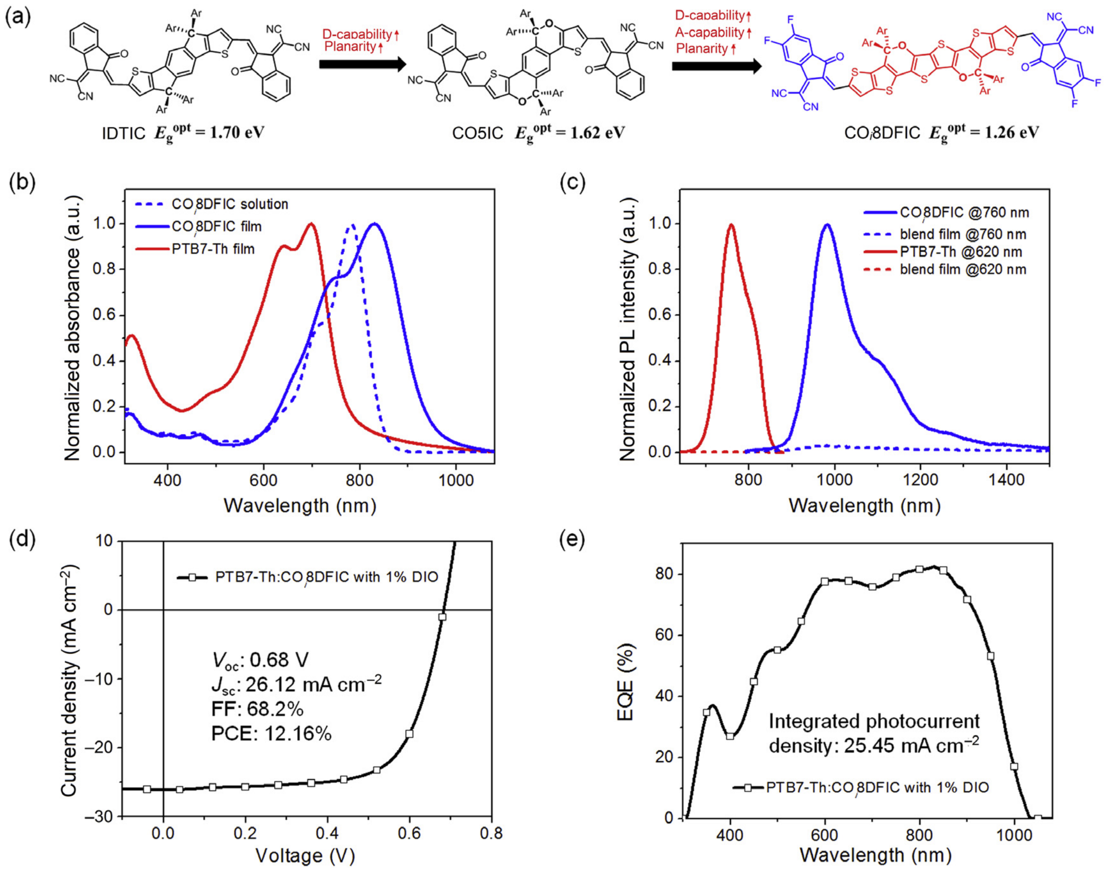

Fig. 1. (Color online) A highly efficient low-bandgap nonfullerene acceptor (CO*i*8DFIC). (a) The structures of IDTIC, CO5IC and CO*i*8DFIC. (b) Absorption spectra for CO*i*8DFIC solution and film, PTB7-Th film. (c) Photoluminescence (PL) quenching between CO*i*8DFIC and PTB7-Th. (d) The *J*-*V* curve for PTB7-Th:CO*i*8DFIC solar cells. (e) The external quantum efficiency (EQE) spectrum for PTB7-Th:CO*i*8DFIC solar cells. D-capability and A-capability stand for electron-donating capability and electron-accepting capability, respectively.

acid-promoted intramolecular transesterification. The addition of four equivalents of Grignard reagent to **3** followed by an intramolecular dehydration cyclization produced CO*i*8 in 84% yield [8]. Deprotonation of CO*i*8 followed by adding *N*,*N*-dimethylformamide gave CO*i*8-CHO in 76% yield. Finally, Knoevenagel condensation of CO*i*8-CHO and DFIC produced CO*i*8DFIC in 60% yield. Nuclear magnetic resonance (NMR) data for CO*i*8DFIC confirmed its chemical structure (Figs. S1–S12 online). High resolution MALDI-TOF mass spectrum gives the expected molecular ion peak for CO*i*8DFIC: $C_{94}H_{76}F_4N_4O_4S_6$ (M^+) (calc. 1,592.4121, found 1,592.4094) (Fig. S13 online).

The absorption spectra for CO*i*8DFIC and PTB7-Th are shown in Fig. 1b. From solution to film, the absorption peak for CO*i*8DFIC shifts from 781 to 830 nm. The large redshift (~50 nm) suggests strong *J*-aggregation of CO*i*8DFIC molecules in solid state. The E_g^{opt} estimated from the absorption onset of CO*i*8DFIC film is 1.26 eV, which is among the lowest values for nonfullerene acceptors to date. The small E_g^{opt} suggests a strong "push-pull" effect between CO*i*8 and DFIC units. CO*i*8DFIC film shows strong absorption at 600–1,000 nm, which is complementary to that of PTB7-Th film (500–800 nm). Thus, the PTB7-Th:CO*i*8DFIC blend may harvest more sunlight to produce high photocurrent. Cyclic voltammetry measurements indicate that the highest occupied molecular (HOMO) and lowest unoccupied molecular (LUMO) levels for CO*i*8-DFIC are −5.50 and −3.88 eV, respectively, and those for PTB7-Th are −5.39 and −3.12 eV, respectively (Fig. S14 online). The relatively large LUMO offset (0.76 eV) between PTB7-Th and CO*i*8DFIC suggests that CO*i*8DFIC could dissociate PTB7-Th's excitons efficiently. Indeed, over 99% PL of PTB7-Th (λ_{max} = 759 nm) was quenched by CO*i*8DFIC in PTB7-Th:CO*i*8DFIC blend film (Fig. 1c). Interestingly, although the HOMO offset is only 0.11 eV, 97% PL of CO*i*8DFIC (λ_{max} = 982 nm) was quenched by PTB7-Th, indicating that the hole transfer from CO*i*8DFIC to PTB7-Th is also efficient.

Bulk heterojunction solar cells with a structure of ITO/ZnO/PTB7-Th:CO*i*8DFIC/MoO_3/Ag were made [9]. The *J*-*V* curve and EQE spectrum are shown in Fig. 1d and e, respectively. The best PTB7-Th:CO*i*8DFIC cells gave a PCE of 12.16%, with an open-circuit voltage (V_{oc}) of 0.68 V, a J_{sc} of 26.12 mA cm^{-2} and a fill factor (FF) of 68.2%. These cells possess a D:A ratio of 1:1 (*w*/*w*), an active layer thickness of 114 nm and 1 vol% 1,8-diiodooctane (DIO) as the additive (Tables S1–S3 online). To the best of our knowledge, 26.12 mA cm^{-2} J_{sc} is the highest value for organic solar cells to date. The high J_{sc} results from the matchups of energy levels and light absorption for donor and acceptor. PTB7-Th:CO*i*8DFIC cells show a broad EQE spectrum and give over 70% EQE at 565–909 nm (Fig. 1e). The maximum EQE of 83% locates at 830 nm, corresponding to the absorption peak wavelength of CO*i*8DFIC. Both PTB7-Th and CO*i*8DFIC contribute photocurrent significantly, indicating that electron/hole transfer between acceptor and donor are quite efficient. The integrated current density from EQE spectrum is 25.45 mA cm^{-2}.

The solar cells without DIO gave lower J_{sc} and FF of 22.83 mA cm^{-2} and 61.8%, respectively, leading to a reduced PCE of 9.93% (Table S3 online). To understand the effect of DIO on device performance, we studied the morphology of the active layer by using atomic force microscope (AFM) and transmission electron microscope (TEM) (Fig. S15 online). After adding DIO, the active layer became rougher, with root-mean-square roughness increasing from 0.98 to 1.40 nm. Clear nanofiber structures with a diameter of ~15 nm can be observed in the film with DIO. TEM image for the film with DIO also shows clear nanofiber structures. These results indicate that DIO can help PTB7-Th and CO$_i$8DFIC to mix in a good way and to build up an effective three-dimensional (3D) passage for the free charge carriers, thus enhancing J_{sc} and FF. We measured the hole and electron mobilities (μ_h and μ_e) by using space charge limited current (SCLC) method (Figs. S16, S17 and Table S4 online). After adding 1 vol% DIO, μ_h increased from 3.70×10^{-4} to 6.82×10^{-4} cm^2 V^{-1} s^{-1} for PTB7-Th, and μ_e increased from 1.55×10^{-5} to 3.91×10^{-5} cm^2 V^{-1} s^{-1} for CO$_i$8DFIC. DIO not only improves charge carrier mobilities but also leads to more balanced charge transport in the active layer, which are beneficial to J_{sc} and FF. We also studied bimolecular recombination by plotting J_{sc} against light intensity (P_{light}). The data were fitted to a power law: $J_{sc} \propto P_{light}^{\alpha}$. The α values for PTB7-Th:CO$_i$8DFIC solar cells without and with 1 vol% DIO are 0.980 and 0.998, respectively, suggesting less bimolecular recombination in the latter (Fig. S18 online) [10].

The molecular packing and orientation were studied by using grazing-incidence wide-angle X-ray scattering (GIWAXS). Pure PTB7-Th film showed a (1 0 0) lamellae stacking peak at 0.26 Å^{-1} in the in-plane direction and a (0 1 0) π–π stacking peak at 1.60 Å^{-1} in the out-of-plane direction, suggesting that PTB7-Th prefers to choose a face-on orientation (Fig. S19 online). For CO$_i$8DFIC film, a π–π stacking peak at 1.70 Å^{-1} was observed in the out-of-plane direction, corresponding to a *d*-spacing of 3.69 Å. Peaks at 0.42 and 0.64 Å^{-1} were observed in the out-of-plane profiles of CO$_i$8DFIC, which might originate from alkyl packing (Fig. S19 online). PTB7-Th:CO$_i$8DFIC blend film without DIO showed dominant features of PTB7-Th, while the π–π stacking peak shifts to 1.67 Å^{-1}. When DIO was used, the π–π stacking peak shifts to 1.70 Å^{-1}, indicating that CO$_i$8-DFIC makes an important contribution (Fig. S20 online). Thus DIO might promote the crystallization of CO$_i$8DFIC to improve electron mobility. The phase separation in PTB7-Th:CO$_i$8DFIC blend films was studied by using resonant soft X-ray scattering (RSoXS). The blend film without DIO showed a quick decay, suggesting no pronounced phase separation. When DIO was added, the scattering in high q region intensified, suggesting that the nanoscale phases became less dispersive (Fig. S20 online). This morphology might result from enhanced crystallization, which improves charge carrier mobilities and FF for solar cells.

In summary, we developed a highly efficient A-D-A nonfullerene acceptor, CO$_i$8DFIC, by assembling an electron-donating CO-bridged ladder-type unit (CO$_i$8) and two electron-accepting end groups (DFIC). CO$_i$8DFIC possesses a narrow optical bandgap of 1.26 eV and can absorb 600–1,000 nm sunlight. Solar cells using PTB7-Th as the donor and CO$_i$8DFIC as the acceptor gave a J_{sc} of 26.12 mA cm^{-2} and a decent PCE of 12.16%. CO$_i$8DFIC proves to be an excellent nonfullerene acceptor, and we will apply it to tandem solar cells and semi-transparent solar cells.

Conflict of interest

The authors declare that they have no conflict of interest.

Acknowledgments

This work was supported by the National Natural Science Foundation of China (U1401244, 21374025, 21372053, 21572041, and 51503050), the National Key Research and Development Program of China (2017YFA0206600), the State Key Laboratory of Luminescent Materials and Devices (2016-skllmd-05) and the Youth Association for Promoting Innovation (CAS). T.P. Russell also thanks the U.S. Office of Naval Research (N00014-15-1-2244) for financial support. Portions of this research were carried out on beamline 11-3 at Stanford Synchrotron Radiation Laboratory, and beamline 7.3.3 and 11.0.1.2 at Lawrence Berkeley National Laboratory.

Appendix A. Supplementary data

Supplementary data associated with this article can be found, in the online version, at https://doi.org/10.1016/j.scib.2017.10.017.

References

[1] Baran D, Kirchartz T, Wheeler S, et al. Reduced voltage losses yield 10% efficient fullerene free organic solar cells with >1 V open circuit voltages. Energy Environ Sci 2016;9:3783–93.

[2] Zhao W, Li S, Yao H, et al. Molecular optimization enables over 13% efficiency in organic solar cells. J Am Chem Soc 2017;139:7148–51.

[3] Lin Y, Wang J, Zhang ZG, et al. An electron acceptor challenging fullerenes for efficient polymer solar cells. Adv Mater 2015;27:1170–4.

[4] Yao H, Cui Y, Yu R, et al. Design, synthesis, and photovoltaic characterization of a small molecular acceptor with an ultra-narrow band gap. Angew Chem Int Ed 2017;56:3045–9.

[5] Cui Y, Yao H, Gao B, et al. Fine-tuned photoactive and interconnection layers for achieving over 13% efficiency in a fullerene-free tandem organic solar cell. J Am Chem Soc 2017;139:7302–9.

[6] Wang W, Yan C, Lau TK, et al. Fused hexacyclic nonfullerene acceptor with strong near-infrared absorption for semitransparent organic solar cells with 9.77% efficiency. Adv Mater 2017;29:1701308.

[7] Xiao Z, Liu F, Geng X, et al. A carbon-oxygen-bridged ladder-type building block for efficient donor and acceptor materials used in organic solar cells. Sci Bull 2017;62:1331–6.

[8] Dou L, Chen CC, Yoshimura K, et al. Synthesis of 5*H*-dithieno[3,2-*b*:2′,3′-*d*]pyran as an electron-rich building block for donor-acceptor type low-bandgap polymers. Macromolecules 2013;46:3384–90.

[9] Xiao Z, Geng X, He D, et al. Development of isomer-free fullerene bisadducts for efficient polymer solar cells. Energy Environ Sci 2016;9:2114–21.

[10] An M, Xie F, Geng X, et al. A high-performance D-A copolymer based on dithieno[3,2-*b*:2′,3′-*d*]pyridin-5(4*H*)-one unit compatible with fullerene and nonfullerene acceptors in solar cells. Adv Energy Mater 2017;7:1602509.